Application of point diffraction interferometry for middle spatial frequency roughness detection

M. V. Svechnikov,* N. I. Chkhalo, M. N. Toropov, N. N. Salashchenko, and M. V. Zorina

Institute for Physics of Microstructures of RAS, Nizhny Novgorod 603950, Russia

**Corresponding author: svch1991@gmail.com*

Received October 24, 2014; revised November 25, 2014; accepted November 30, 2014;
posted December 1, 2014 (Doc. ID 225719); published January 7, 2015

The possibilities of applying the point diffraction interferometry (PDI) method for the detection of the middle spatial frequency roughness of superpolished optical surfaces are analyzed. The point source used in the experiment is based on a single mode optical fiber with the subwavelength exit aperture size, which is about 0.25 μm. In a numerical aperture of 0.01 the reference wave root-mean-square deformation is less than 0.005 nm. It is theoretically shown that the possible diffraction-limited lateral resolution of PDI while measuring a spherical substrate of 100 mm curvature radius is about 8 μm. The experiment demonstrated the possibility of obtaining roughness spectra in the range 0.001–0.05 μm^{-1}. The surface map obtained by PDI, and the roughness spectra obtained by both the PDI and atomic-force microscopy methods are shown.

OCIS codes: (120.4800) Optical standards and testing; (240.5770) Roughness; (120.6660) Surface measurements, roughness.

http://dx.doi.org/10.1364/OL.40.000159

In connection with the progress in manufacturing normal incidence multilayer mirrors for extreme ultraviolet (EUV) and soft x-ray (SXR) radiation there is a real possibility of creating imaging optics with diffraction-limited spatial resolution that are needed, for example, in EUV projection lithography [1] at a wavelength of 13.5 nm. The main obstacle to the transition to shorter wavelengths, that are in demand in BEUV (beyond extreme ultraviolet) lithography [2] and the microscopy of "carbon" and "water" transparency windows (wavelengths of 2.3–5 nm) [3], is the complexity in manufacturing substrates with integral roughness at a level of one angstrom at the lateral dimension range of 1 nm–1 mm. A necessary condition for the solution of this problem, beside development of optical surfaces superpolishing technology, is the availability of adequate methods for measuring such a small roughness in the region of the spatial frequencies mentioned above.

The special effect on the utmost resolution of optical elements and systems has so-called middle spatial frequency roughness (MSFR, 0.001–1 μm^{-1}) as waves, scattered at such a roughness, are within the Bragg peak and, thus, gain interferential amplification, leading to a blurring of the edges of the image.

The most used tools for MSFR measurements are the white light interferometer (WLI) [4] and atomic-force microscope (AFM) [5]. A number of papers report good agreement between these two methods [6,7], but there is also evidence of significant discrepancies [8]. It is noted that the results of the measurement of supersmooth surfaces, when WLIs are used, depend, to a considerable degree, on the set reference and the lens and on the level of mechanical vibrations, as well as the accuracy of the piezo-scanner calibration. Thus, it is strongly recommended that the obtained result are verified by independent measurements, based on other physical or technical principles.

To measure roughness in the range of spatial frequencies from 0.01 μm^{-1} or higher (lateral dimensions less than 100 μm) such methods as AFM and x-ray diffuse scattering (XRDS) analysis [9] are used. X-ray scattering may be described by electrodynamics laws, and its measurements are well reproducible in the laboratory, so that, under certain conditions, this method can be attributed to the "first-principle." Many studies (for example, [8–10]) ensure that AFM and XRDS measurements of plane specimens have a good agreement. Since the XRDS technique is almost inapplicable for the study of curved surfaces (i.e., surfaces of almost all optics imaging elements), then, as a standard method, AFM is also used.

In the low-frequency part of the MSFR, 0.001–0.01 μm^{-1} (lateral dimensions 1 mm–100 μm), currently there is no other way, beside WLI, of directly determining the roughness. Nevertheless, the need for an alternative method for the mentioned MSFR subrange is unquestionable, especially when measuring supersmooth substrates with a root-mean-square roughness of less than one nanometer.

In this Letter, we consider the possibility of applying the point diffraction interferometry (PDI) method, which is widely used for measuring LSFR, as a reference, with respect to the WLI, that allows the quality of the measurements to be controlled exactly in the range of 0.001–0.01 μm^{-1}. As a criterion of the adequacy of the method, the coincidence between the AFM and PDI data in the intersection of their working frequency bands was chosen.

A typical scheme of the point diffraction interferometer is shown in Fig. 1. Quasi-spherical wave source (4) illuminates the investigated concave spherical surface (5) and CCD (charge-coupled device) matrix (7). As a source of quasi-spherical waves, a single mode optical fiber with a subwavelength aperture is used [11]. Light reflects from the surface under study, focuses on the plane mirror (3) near the source and rereflects to the CCD matrix, where it interferes with the quasi-spherical wave from the source. As a result, interference fringes like two adjacent point sources are seen.

Experiments were conducted at the interferometer, whose photo is shown in Fig. 2.

All the elements are arranged on an optical table, with air and spring damping for vibration isolation, under a

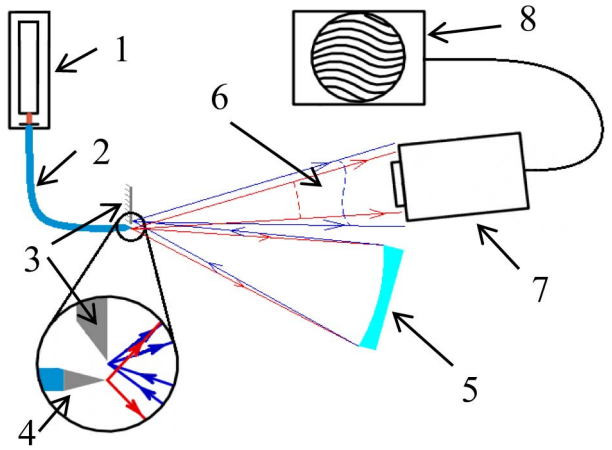

Fig. 1. PDI scheme. 1—laser, 2—optical fiber, 3—plane mirror, 4—quasi-spherical wave source, 5—spherical substrate/mirror under study, 6—interfering wave fronts, 7—CCD camera, and 8—PC.

transparent cover to protect against air currents. The interferometer is located in an isolated room with temperature stabilization.

The quality of the reference wave, produced by the mentioned subwavelength source, was investigated in [12]. The maximal size of investigated area was chosen about 2 mm, so, since curvature radius is 100 mm (see below), the used NA is about 0.01 and a root-mean-square of wave front deformations is less than 0.005 nm.

The PDI parameters for the experiment and for the calculations are presented in Table 1.

We can make certain estimations of the possibility of observing roughness using PDI. Visible light is electromagnetic radiation, characterized by diffraction, i.e., changes in the spatial distribution of the field in the process of propagation. Light, reflected from the mirror, has information about wave front phase shifts, but this information is lost during propagating. The influence of the diffraction can be estimated as follows: the size of the round beam in the far field (Fraunhofer zone) is characterized by the formula $0.61(\lambda/a) * z$, where λ is the wavelength, a is the initial diameter of the beam, and z is the distance to the screen. It is easy to show

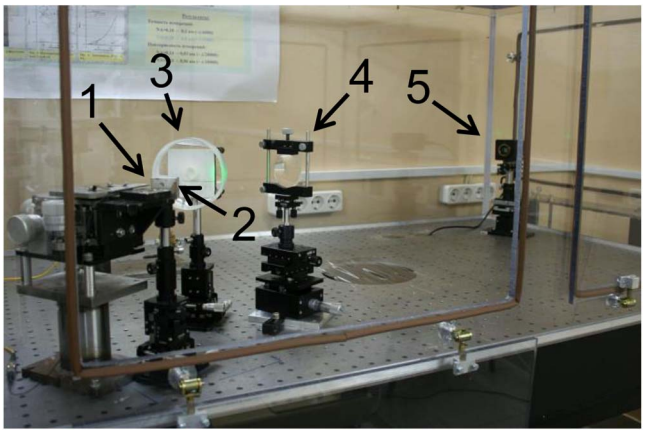

Fig. 2. Photo of the interferometer. 1—quasi-spherical wave source, 2—plane mirror (rear view), 3—quartz substrate, 4—imaging lens, and 5—CCD camera.

Table 1. Parameters of the PDI

PDI wavelength	532 nm
Investigated surface curvature radius	100 mm
Lens focal length	250 mm
Lens diameter	50 mm
Distance from lens to CCD	875 mm
Magnification factor (MF) of optical system	2.8; 12.5; 2.5 (for calculations)
Investigated area	1.66 mm (MF 2.8) 0.38 mm (MF 12.5) 34.6 μm (for calculations)

that, even at a distance of a few tens of millimeters, the diffraction broadening of the beam will be significantly greater than its initial size, corresponding to the lateral roughness dimensions of interest.

Thus, to observe mirror roughness of lateral size 1 mm–10 μm, it is necessary to add to the interferometer (see Fig. 1) an imaging lens or an objective between the source (4) and CCD (7) to form a surface area image of about 2 mm on the 5×7 mm CCD matrix. This also must hold the diffraction limit of less than 10 μm. To obtain such an image, the substrate and CCD should be located at conjugate planes of the imaging system.

The imaging system can introduce some additional distortion to the wave fronts, passing through it, but these aberrations can be taken into consideration by using a scheme with two sources, similar to Young's experiment [11].

Calculation of the interferometer diffraction resolution was carried out by computation of the field using Kirchhoff diffraction theory:

$$U(P) = \frac{-ik}{4\pi}\frac{e^{-ikr}}{R}\iint_{S_1} A(x,y)\frac{e^{iks+i\varphi(x,y)}}{s}(1+\cos\chi)\mathrm{d}S, \tag{1}$$

where R is the substrate curvature radius, $A(x,y)$ the amplitude distribution on the substrate, $\varphi(x,y)$ is the phase distribution on the substrate, s the distance from the point of integration to the point P where the field is calculated, χ is the angle between the normal to the substrate at the point of integration and the direction to point P, and $U(P)$ is the scalar field amplitude. The integration is over the entire surface of the substrate. Scalar theory is applicable here because of small NA in the optical elements (NA < 0.05) and almost normal light incidence.

To find the utmost resolution of the method, we specified the phase distribution near the substrate (amplitude was considered to be a constant), calculated the field in the image plane and summed it with a field of reference wave for the interference pattern. Being deciphered, the resulting interferograms allow comparison of the specified and restored reliefs to be undertaken and a preliminary conclusion about the resolution of this relief to be drawn. As relief, we requested a one-dimensional sine wave with amplitude of 5 nm and different periods. The period in which the amplitude of the reconstructed sine wave fell twice was adopted as the diffraction limit.

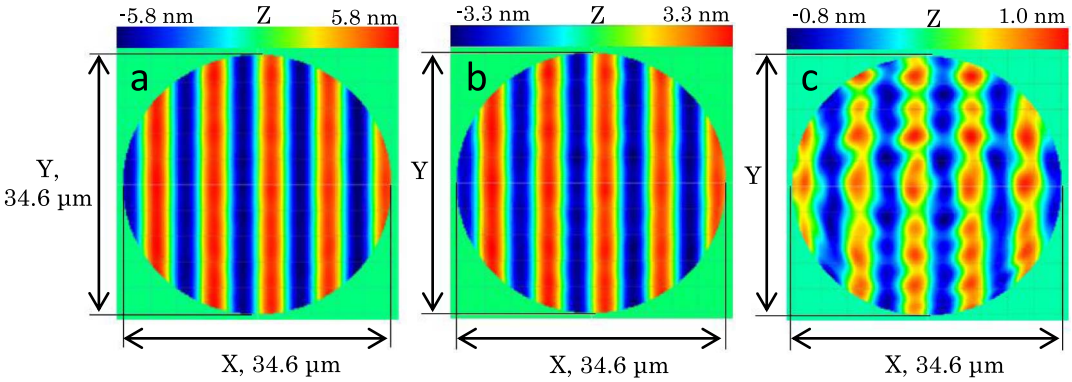

Fig. 3. Reconstructed relief. The period: (a) 7.7 µm, (b) 7.5 µm, and (c) 7.3 µm. Specified amplitude is 5 nm. Reconstructed amplitude: (a) 5.8 nm, (b) 3.3 nm, and (c) 0.9 nm. The color scale of the profile height Z(X,Y) is given at the top of each image.

Figure 3 shows examples of a one-dimensional sine relief, reconstructed from simulated interferograms. When reducing the period of relief, the reconstructed amplitude reduces too; moreover, the relief height dependence of the Y coordinate, associated with the reconstruction error, may appear. The resolution of the system, being defined by the twofold fall in the restored relief amplitude, is 7.5 µm.

The resolution of the same system by the conventional Rayleigh criterion for coherent light is $0.77\lambda_0/(n * \sin\theta) = 5.7$ µm. As far as the AFM allows reliable measurements in the frame of up to 60×60 µm, the resulting resolution limit of the optical system provides for sufficient intersection of the PDI and AFM frequency ranges.

The interferometer is configured so that about 20 interference fringes appeared on the CCD matrix. This number is the trade-off between the number of points at which wave front deformation will be calculated (the more fringes the better), and an increase in accuracy of the coordinates of these points (the less fringes the better). The interference pattern is decoded, and the outputs show the map of deformations as a set of approximating functions—Zernike polynomials (see, for example, [13]). For greater precision, several maps, built of interferograms, phase-shifted relatively to each other, are averaged. Using the deformation map, the roughness spectral function is constructed.

Figure 4 shows the surface topography of the two areas of 1.66 mm (b) and 0.38 mm (d). These are obtained with the magnification factors of 2.8 and 12.5, respectively, and represented as sets of Zernike polynomials:

$$\{R_n^m \cos m\varphi, R_n^m \sin m\varphi,$$
$$n = 2\ldots 68, m = -n\ldots n, m \pm n \leq 68\}.$$

Figure 5 shows the spectral curves of the mirror surface roughness, measured by PDI and AFM. Two curves that lie in the range 0.0017–0.1 µm^{-1} are constructed on the square surface area with a side of 1.17 mm, inscribed in a circle area in Fig. 4(b). They are averaged over the rows (columns) one-dimensional PSD (power spectral density) functions in two orthogonally related directions x and y:

$$\mathrm{PSD}_{1D}(\nu_x) = \frac{1}{L_y}\int\left(\frac{1}{2\pi}\int C(\vec{r})e^{-2\pi i x \nu_x}\mathrm{d}x\right)\mathrm{d}y, \quad (2)$$

where $C(\vec{r})$ is a correlation function, L_y is the y size.

The coincidence of the effective roughness in two directions shows roughness isotropy. Similarly, PSDs in the range 0.0075–0.51 µm^{-1} are obtained by the PDI on a square area of 0.268 mm^2, with a magnification factor of 12.5 [central part of Fig. 4(d)]. The higher-frequency PSDs are obtained with AFM over 60, 40, and 2 µm square frames.

As seen in Fig. 5, PSDs obtained by the PDI method bridged the problematic part of the roughness spectrum at 0.001–0.01 µm^{-1} and consistently connected with the

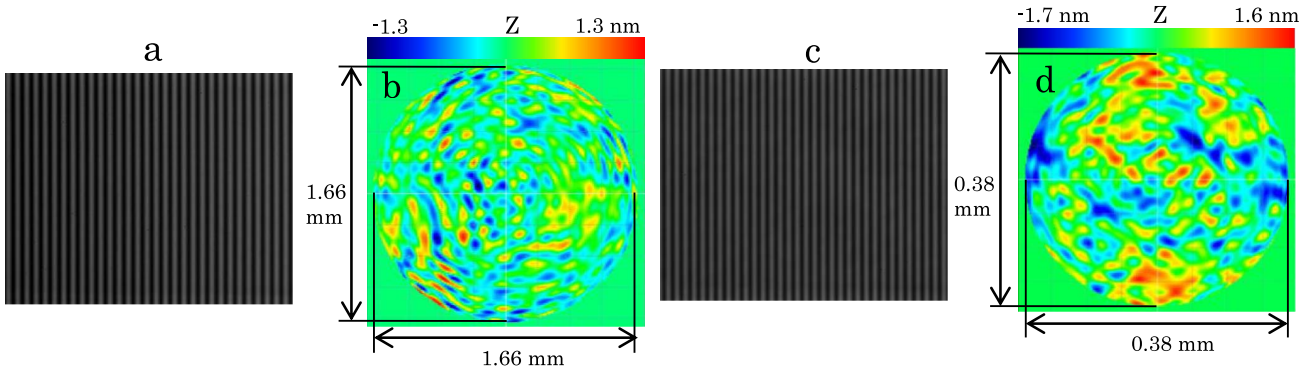

Fig. 4. Interferograms and reconstructed maps of two surface areas. The map (b) is obtained from the interferogram (a) with the magnification factor of optical system of 2.8, and map (d) is obtained from the interferogram (c) with the factor 12.5. The color scale of the profile height Z(X,Y) is given at the top of map images.

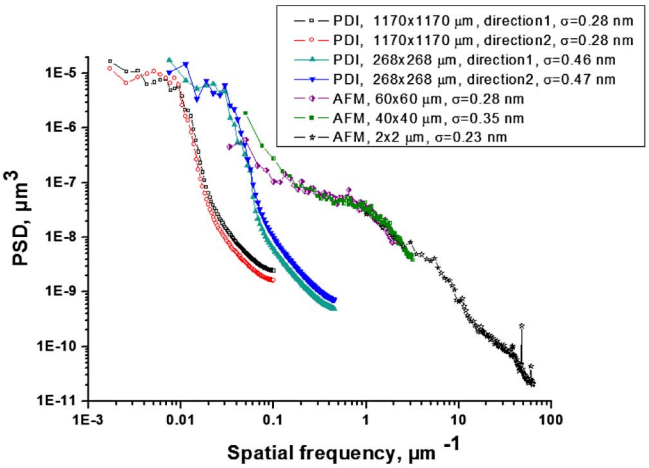

Fig. 5. PSD functions of a spherical mirror with curvature radius 100 mm. Effective roughness by PDI in the range 0.0017–0.05 μm^{-1} is 0.8 nm and by AFM in the range 0.05–70 μm^{-1} is 0.5 nm.

AFM curves. Effective root-mean-square roughness of the substrate is 1.3 nm in the range 0.0017–70 μm^{-1}. As far as we propose the PDI for angstrom-smooth surfaces, it must be tested on corresponding samples, but before this the reliability of spatial resolution must be approved.

The calculation showed that the PDI method can be a tool for determining the MSFR. In the measurement of standard concave substrates and mirrors, used in SXR microscopy and lithography, the PDI diffraction limit is less than 10 μm. It is sufficient to compare the results of the PDI and AFM measurements.

The experiment demonstrated the possibility of obtaining roughness spectra in the range 0.001–0.05 μm^{-1}. The diffraction-limited resolution was not achieved because of the rapid decrease in spatial spectra in the high-frequency direction that is, in turn, related to the surface topography representation as a set of Zernike polynomials. Narrow spectral composition of such a representation leads to the need to rebuild the interferometer to obtain greater magnification and, consequently, higher-frequency roughness spectra.

The problem of too narrow a measurement spectrum can be solved by abandoning the approximating functions, and, for example, applying the "phase" method to determine the wave front deformation. This method consists of obtaining a large number of interferograms with a known phase shift between them and the total phase shift of 2π and analysis of intensity trends in each pixel of the CCD matrix from interferogram to interferogram. The result of such processing is a raster map with a number of points equal to the number of enabled pixels of the matrix (in each coordinate). A similar method is implemented in WLI, with the difference that, in each pixel, the peak of interference intensity is sought while the scanning objective is moving through all the level differences of the relief, including its slope. At present, we use the "phase" method to determine the global deformations (aberrations) of substrates and mirrors and are studying the possibility of applying it in roughness determination.

This work was supported by a Russian fund for basic research by the Ministry of Science and Education of Russia.

References

1. C. Wagner and N. Harned, Nat. Photonics **4**, 24 (2010).
2. J. Kirz, C. Jacobsen, and M. Howells, Q. Rev. Biophys. **28**, 33 (1995).
3. I. Artyukov, Y. Bugayev, O. Devizenko, E. Gullikson, V. Kondratenko, and A. Vinogradov, Opt. Lett. **34**, 2930 (2009).
4. R. Blunt, "White light interferometry—a production worthy technique for measuring surface roughness on semiconductor wafers," *CEMANTECH Conference*, Vancouver, Canada, Apr. 24–27, 2006, pp. 59–62.
5. J. E. Griffith and D. A. Grigg, J. Appl. Phys. **74**, R83 (1993).
6. V. V. Azarova, V. G. Dmitriev, Yu. N. Lokhov, and K. N. Malitskii, J. Opt. Technol. **69**, 125 (2002).
7. D. Martinez-Galarce, R. Soufli, D. L. Windt, M. Bruner, E. Gullikson, Sh. Khatri, E. Spiller, J. C. Robinson, Sh. Baker, and E. Prast, Opt. Eng. **52**, 095102 (2013).
8. N. I. Chkhalo, S. A. Churin, A. E. Pestov, N. N. Salashchenko, Yu. A. Vainer, and M. V. Zorina, Opt. Express **22**, 20094 (2014).
9. V. Holy and T. Baumbach, Phys. Rev. B **49**, 10668 (1994).
10. I. V. Kozhevnikov and M. V. Pyatakhin, J. X-Ray Sci. Technol. **8**, 253 (2000).
11. N. I. Chkhalo, A. Yu. Klimov, V. V. Rogov, N. N. Salashchenko, and M. N. Toropov, Rev. Sci. Instrum. **79**, 033107 (2008).
12. N. N. Salashchenko, M. N. Toporov, and N. I. Chkhalo, Bull. Russ. Acad. Sci. Phys. **74**, 53 (2010).
13. D. Malacara, M. Servin, and Z. Malacara, in *Interferogram Analysis for Optical Testing*, 2nd ed. (Taylor & Francis, 2005), pp. 137–167.